

The prediction of shallow landslide location and size using a multidimensional landslide analysis in a digital terrain model

W.E. Dietrich

Department of Earth & Planetary Science, University of California, Berkeley, CA 94720-4767;

Department of Geography, University of California, Berkeley, CA 94720-4740

J. McKean

US Forest Service, Rocky Mountain Research Station, Boise Idaho, 83702

D. Bellugi & T. Perron

Department of Earth & Planetary Science, University of California, Berkeley, CA 94720-4767

Keywords: shallow landslide size, slope stability, digital terrain model

ABSTRACT: Shallow landslides on steep slopes often mobilize as debris flows. The size of the landslide controls the initial size of the debris flows, defines the sediment discharge to the channel network, affects rates and scales of landform development, and influences the relative hazard potential. Currently the common practice in digital terrain-based models is to set the landslide size equal to an arbitrarily chosen grid cell dimension. Here we apply a multidimensional landslide model that assumes that a soil block fails as a rigid mass when downslope forces overcome cohesive and frictional resistances developed over the area of the slide base and lateral walls. We find that for a specified block width and length, there is a range of soil depth at which failure may occur. For low lateral root strength, basal root cohesion prevents shallow failures and lateral earth pressure prevents deep failures. As lateral root strength increases, the range of instability narrows until all soil depths are stable. We propose that in the field, failure location and size are largely controlled by the spatial structure of soil depth, topography, vegetation and shallow subsurface flow (and corresponding pore pressure development). To explore how this structure affects slope stability, we use a stochastic soil production model coupled with a nonlinear slope dependent flux model to predict the spatial variation in soil depth across an inclined planar hillslope, and then model how this depth variation affects the location and size of soil landslides. We use a search algorithm to identify the shapes and sizes of all soil blocks that would fail, as well as the least stable block. Our model is a first step toward a procedure that uses the spatial structure of controlling factors to predict landslide size, as compared to the current practice of assigning sizes based on grid resolution.

1 INTRODUCTION

In steep landscapes, shallow landslides that commonly involve only the colluvial soil mantle can be the primary sources of debris flows that rush downslope, carve valleys into bedrock, and create destructive, coarse-grained pulses of sediment. Two key aspects of shallow landslides that affect their mobility, geomorphic significance, and resulting downstream hazard, are their location and their size. Depending on whether a slide initiates on a planar side slope near a channel or at the steep headwall of a tributary, the travel distance, bulking-up potential, and downstream effects may differ greatly (e.g., Benda & Cundy 1990; Fannin & Wise 2001). Landslide size strongly affects sediment discharge to channels and the scale of local morphologic change. We currently lack, however, a mechanistic model for predicting shallow landslide size across landscapes. This inhibits our ability to formulate and apply mechanistic models for landslide flux and surface erosion.

Thus, landscape evolution models for steep landscapes currently characterize the effects of landsliding through either a nonlinear, slope-dependent flux law (e.g., Howard 1994), or grid-based infinite slope calculations in which size is dictated by arbitrary grid cell dimensions (e.g., Tucker & Bras 1998).

For practical purposes of landslide hazard delineation, it may be that various empirical procedures for constructing hazards maps are sufficient (e.g., see the summary in Soeters & van Westen 1996). Our goals are different here, as we eventually wish to predict through time and various climate and landuse conditions the flux of landslide-generated sediment to channels. We also want to gain insight in how to construct a shallow landslide geomorphic transport law (Dietrich et al. 2003) that can be used over long time scales to predict the form and evolution of landscapes. These goals require a process-based approach, but one that can be applied over large areas and through long time periods on an evolving land surface. As such, we wish to explore models that are sufficiently mechanistic that they have meaningful parameters and can be tested to some degree, but not so deeply mechanistic that their application across large landscapes and long time periods is impractical.



Figure 1. Shallow landslides on hillslopes near Briones, California, showing a range of size and location (note that the unvegetated scars partly include the runout portion of the slide; scene width is about 300m).

Field observations on shallow landslides show that even for a single storm, in a relatively uniform vegetation cover and a single rock type, landslide size varies considerably (Fig. 1). Such landslides, however, are rarely wider than they are long, and seldom exceed a width of 10s of meters. Failures typically occur near the soil-bedrock interface and soil thickness is commonly 1m or less, although thicknesses in hollows of colluvial fills can approach several meters. We typically find that soils on steep slopes are relatively coarse (gravel and sand abundant), have high angles of internal friction and are cohesionless. On vegetated landscapes we rarely find roots penetrating the basal slide plane of sites that have failed, but they are common along the marginal walls, with many of the roots broken rather than pulled out (e.g., Schmidt et al. 2001). There is some evidence that these landslides vary with vegetation type (e.g., Gabet & Dunne 1992). Location also varies, although there is a tendency for soil landslides to be more common in topographically convergent areas (e.g., Reneau & Dietrich 1987).

Digital elevation models are now commonly used in landslide potential mapping, either as a source of topographic data for statistical delineations (e.g., Schulz 2006), or as surfaces on which local slope stability calculations are performed to determine relative instability (e.g., Okimura 1994; Montgomery & Dietrich 1994; Pack et al. 1998; Xie et al. 2004). Increasingly, models that exploit these data are being developed to predict the spatial distribution of potential landslide areas across catchments (e.g., Montgomery & Dietrich 1994; Xie et al. 2006; Claessens et al. 2005; Tarolli & Tarboton 2006). The most common approach has been to use some form of the infinite slope equation on a point-by-point basis, in which properties such as soil depth, root strength, and pore pressure are varied either statistically (Pack et al. 1998), empirically (Wu and Sidle 1995), or mechanistically (Dietrich et al. 2006; Claessens et al. 2005). Soil depth is often inferred from existing maps, although a process-based prediction of soil thickness variation may give a more realistic estimate of local soil thickness variation (Dietrich et al. 1995; Heimsath et al. 2001). Such models are usually deterministic, yet soil production and transport are highly stochastic, and local soil depth variations can be accordingly large (Heimsath et al. 2001; Schmidt 1999). Root strength has been correlated with canopy type and age (since cutting or burning) to show the effects of forest management on slope stability changes (Burroughs & Thomas 1977; Gray & Megahan 1981; Ziemer, 1981; Wu & Sidle 1995; Montgomery et al. 2000; Schmidt et al. 2001; Roering et al. 2003). The effect of root strength is normally included as a basal cohesion term in the infinite slope expression, although field observations (e.g., Schmidt et al. 2001) often indicate that the lateral root strength matters most. Burroughs (1984) developed force balance expressions that explicitly include root strength and lateral earth pressure terms in a full three-dimensional formulation of the shallow slope stability problem for the case of failure parallel to the ground surface. Reneau & Dietrich (1987), Schmidt et al. (2001) and Casadei & Dietrich (2003) have proposed reduced versions of this formulation in which lateral earth pressure terms were ignored, and the focus was on predicting either the relative saturation at failure (Schmidt et al. 2001) or the width of the landslide scar (Reneau & Dietrich 1987; Casadei & Dietrich 2003). While this simplification enables analytical results, it is not clear whether in shallow landslides the lateral stress terms can be ignored without significantly affecting the model results.

Most efforts to exploit digital terrain models for shallow landslide prediction have introduced first steady state, and then dynamic, hydrologic models to estimate local pore pressure driving instability (e.g., Montgomery & Dietrich 1994; Pack et al. 1998; Wu & Sidle 1995; Casadei et al. 2003; Iverson 2000; Rosso et al. 2006). While the full three-dimensional, variably saturated flow calculation can be performed for small areas (e.g., Ebel et al. 2007a, b), approximations have been sought for landslide modeling over large areas, with increasing effort to introduce pore pressure dynamics in response to storms. The most advanced approximate modeling (Iverson 2000) enables treatment of both the lateral subsurface flow and the dynamic passage of vertical flux on pore pressure development.

While important progress has been made in the mechanistic treatment of the drivers and controls on slope instability, there remains the problem that landslide modeling is still done on a grid (or polygon) basis such that size is an artifact of grid dimension (e.g., Tucker & Bras 1998). Okimura (1994), in a pioneering analysis of three-dimensional slope stability, proposed a method of columns approach which first identified a least stable cell, and then evaluated the critical slide mass for a rectangular failure oriented downslope in which a tension crack is assumed at one side and at the upper of the potential slide mass. Xie et al. (2006) have implemented various three dimensional slope stability models in a GIS framework for site specific investigations. Casadei & Dietrich (2003) proposed that landslide size should be set by local combinations of root strength gaps, elevated soil thickness, high pore pressure and slope steepness. Their simplified model, which ignored lateral earth pressure terms, predicted that landslide size would be smaller for high pore pressure, steeper slopes and lower root strength. They did not attempt to implement their model using digital elevation data.

The next challenge is to build models that use the spatial and temporal variability of factors that control instability to determine unstable areas of the landscape, with minimal influence of grid resolution and orientation. Results, of course, will depend strongly on the accuracy of the digital

elevation data (e.g., Dietrich et al. 2001; Claessens et al. 2005). This is a major task, for not only does it require reliable models or maps of these factors (e.g. soil depth, pore pressure, and root strength), it also requires an algorithm that can find the unstable zones and calculate landslide dimension. Here we take a step in that direction. We first propose a multidimensional slope stability model that explicitly includes effects of lateral earth pressure and cohesion (similar to the model of Burroughs, 1984). Unexpectedly, this model predicts that, for a given lateral root strength, instability is restricted to an intermediate range of soil depth. We then use a simple inclined hillslope with patchy soil thickness to explore how to identify the size of a landslide that occurs in a landscape with spatial variations in soil thickness. Two methods are used. In the first, we calculate the degree of instability for all possible groups of grid cells with convex plan geometry (i.e. no indentations on the boundary) and identify the largest unstable group. In the second, the least stable grid cell is removed, potential upslope instability is recalculated, the next least stable cell is removed, and the procedure is repeated until all remaining cells are stable. Although this initial modeling is promising, the search process is computationally demanding, even for a small area, and methods are needed to create directed searches that minimize iterations.

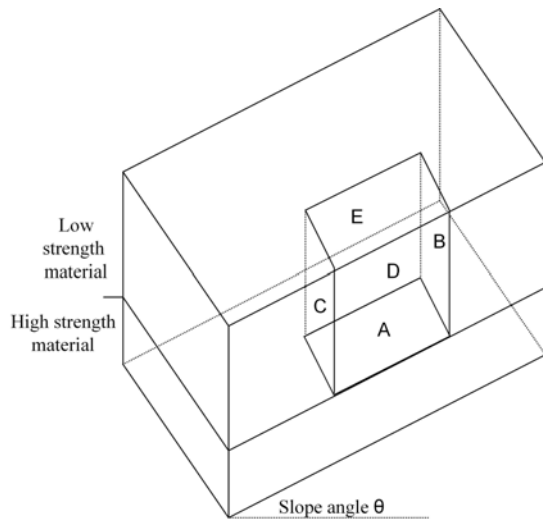


Figure 2. Three dimensional force balance stability analysis of a soil element on a slope. Force A on the element bottom boundary results primarily from the lithostatic stress of the element mass. Forces B and C arise from active and passive earth pressure, respectively, while forces D and E result from at rest earth pressure on the element lateral margins.

2 MULTIDIMENSIONAL SLOPE STABILITY MODEL

We use a simple three-dimensional limit equilibrium force balance on a slope element (Fig. 2) and assume that failure occurs by simultaneous shear on the boundaries of the element, without internal deformation. This is likely incorrect in detail (see Iverson & Reid 1992) but is a necessary simplification at this point. Work is underway to investigate the typical magnitude of error involved in this assumption. Our model is an adaptation of the methods of Hovland (1977) and Arellano and Stark (2000) and considers only translational slides with non-circular failure surfaces. Further work is planned to test and calibrate the model against other failure analyses. No progressive failure with strain softening, pore water pressure dynamics, or other unequal stress-strain behavior is considered. We assume the four lateral boundaries of the element are vertical. The head scarps and two lateral margins of most debris flow failures are often quite steep, in our experience, and typical small deviations from vertical are likely to change calculated boundary forces by only a few percent, much less than other uncertainties in limit equilibrium analyses. However, the boundary across the downslope toe of a slide may have a variety of orientations, dependent particularly on

the prefailure slope morphology. For the present, we assume a simple vertical toe boundary, but plan to investigate this boundary condition more closely in the future. We characterize shear resistance on the two lateral vertical boundaries and base of the element as a result of a combination of cohesion (soil and root cohesion) and friction and describe this strength by the usual Mohr-Coulomb linear, isotropic criterion. We represent frictional resistance on the two lateral vertical boundaries as the depth-averaged earth pressure perpendicular to a boundary multiplied by the tangent of the soil friction angle, ϕ , similar to the work by Burroughs (1984), Arellano & Stark (2000) and Chugh (2003). We further assume the frictional resistances only develop after some finite movement of the slope element; thus each frictional force is initially inclined at an angle ϕ from perpendicular to the element boundaries at the moment of instability. We consider earth pressures from directly uphill and downhill of the analyzed element to cause simple boundary forces on a rigid slope element. The respective boundary earth pressure conditions are indicated in Fig. 2 and the coefficients of active, passive, and at rest earth pressure are all predicted by the conventional formulations: $K_a = \tan^2(45 - \phi/2)$, $K_p = \tan^2(45 + \phi/2)$, $K_o = 1 - \sin \phi$. Presently, we define the basal shear surface at the soil-bedrock boundary which we presume is the position of material shear strength contrast. Research is planned to predict mechanistically the failure depth within a colluvial soil, when soil depths are large. We assume that root cohesion develops from simultaneous tensile failure of all roots crossing the element boundaries (roots do not pull out intact, which would mobilize skin friction rather than tensile strength). Resistance from soil arching between root wads is ignored (Burroughs 1984).

With these assumptions and definitions, we calculate the usual factor-of-safety as the ratio of total available shear force resistance, R , over the necessary force resistance (the driving force), F_d , where R and F_d are defined as:

$$R =$$

$$C_b WL \sec \theta +$$

$$\left[(\rho_s Z - \rho_w h) g WL \pm \frac{1}{2} g (K_a - K_p) (\rho_s Z^2 - \rho_w h^2) W \sin(\phi - \theta) \right] \tan \phi +$$

$$2C_l ZL + K_o g (\rho_s Z^2 - \rho_w h^2) L \cos \phi \tan \phi + \quad (1)$$

$$C_l ZW +$$

$$C_l ZW + \frac{1}{2} K_p g (\rho_s Z^2 - \rho_w h^2) W \cos(\phi - \theta)$$

$$F_d = \rho_s g ZWL \sin \theta + \frac{1}{2} K_a g (\rho_s Z^2 - \rho_w h^2) W \cos(\phi - \theta) \quad (2)$$

and the “ \pm ” sign in line 2 is + if $\phi > \theta$, - if $\phi < \theta$.

Lines 1 and 2 of Eq. 1 represent the resistance on the base of the element, line 3 the resistances on the two lateral sides, line 4 the cohesion on the head scarp, and line 5 the resistance on the downslope slide boundary. L and W (m) are measured horizontally (they are the grid spacing), C_b and C_l (Pa) are the total basal and lateral cohesion from both soil and roots, Z (m) is the vertical soil depth, h (m) is the saturated part of Z , ρ_s and ρ_w (kg/m^3) are the soil and water densities, θ and ϕ (degrees) are the slope and friction angles, g is gravity (m/s^2), and the slope is oriented in the L direction.

3 MODEL FOR SOIL THICKNESS

In order to create the patch variation in soil thickness we use a stochastic soil production and annual soil transport model, building upon our earlier work (Dietrich, et al. 1995). Field observations and cosmogenic radionuclide dating (Heimsath et al. 2001) confirm that the rate of conversion of intact bedrock to mobile soil (typically due to biotic disturbance) declines exponentially with soil depth, and can be expressed as:

$$-\frac{\partial z_b}{\partial t} = \varepsilon e^{-\alpha h} \quad (3)$$

Here z_b (m) is the height of the soil-bedrock boundary above some datum, t is time, ε is the production rate (m/yr) at zero soil thickness, α (1/m) is the rate constant, h (m) is the soil thickness normal to the bedrock boundary. This expression coupled to a soil transport law has been used to predict soil thickness variation across landscapes (e.g., Dietrich et al. 1995; Heimsath, et al. 2001) and compares generally well in predicting thin soils on narrow, strongly curved ridges and thick soils in hollows. Soil production by tree throw and burrowing animals, however, creates large local transient variations in soil thickness that may be of large enough extent to influence slope stability. We suggest that production of soil by tree throw or animal burrowing has some characteristic recurrence interval (N). To model stochastic production at each time step we generate random numbers between 0 and 1 for each cell and when that number is smaller than $1/N$ for the specific N , production occurs. The total soil production will be the time since last production times the term on the right hand side of Eq. 3. The value of N varies with production mechanism from 100s to 1000s of years for tree throw to decadal for animal burrowing.

On an annual basis there is localized production of soil and there is dilational disturbance by smaller scale biotic and abiotic processes that move soil downslope (we are not considering periglacial or salt driven processes). We model annual transport across the entire hillslope using the nonlinear flux equation proposed and quantified by Roering et al. (1999):

$$\tilde{q} = \frac{K \nabla z}{1 - (|\nabla z| / S_c)^2} \quad (4)$$

For this specific modeling exercise we chose parameters that were calibrated for the Oregon Coast Range. We set K equal to 0.0032 (m²/yr) and S_c to 1.25 (m/m) based on Roering et al., (1999), a is set to 0.0003 (1/m) and ε to 0.000268 (m/yr), based on Heimsath et al., (2001), while we picked a recurrence interval N of 1000 years and a cell size of 5 m, which are representative of a tree-throw dominated soil production mechanism.

4 RESULTS

4.1 *Soil thickness and slope stability*

To explore the roles of the various terms in Eq. 1, we divide each term by Eq. 2 to define a factor of safety (FS) and plot the contribution to the total factor of safety in Fig. 3 as a function of soil depth. This illustrates how various strength components contribute to slope stability and create a window of soil depth in which instability can occur. At shallow soil depths, root cohesion through the base creates a high FS. With increasing soil depth, this basal root strength component is diminished until, for a range of soil depths, the FS drops below 1. But with continued increase of soil depth, the lateral frictional resistance relative to the downslope force also increases, eventually raising the FS back above 1. This result differs greatly from the conventional infinite slope analysis

that predicts just decreasing strength with increasing depth as in the case of “Shalstab + Basal” in Fig. 3 where “Shalstab” refers to the coupled shallow subsurface flow and slope stability model described by Montgomery & Dietrich (1994).

In Fig. 4, fields of stable and unstable values of soil depth and lateral root strength are shown for an 8 m by 16 m block under saturated conditions. With no lateral cohesion, the range of soil thickness at which instability occurs is greatest. As lateral root strength increases this range narrows, ultimately preventing instability at any depth. The particular range of soil depths for which instability is possible will vary with relative saturation, hillslope gradient, friction angle and basal root strength. Figs. 3 & 4 taken together illustrate an unexpected finding: instability does not systematically increase with increasing soil depth.

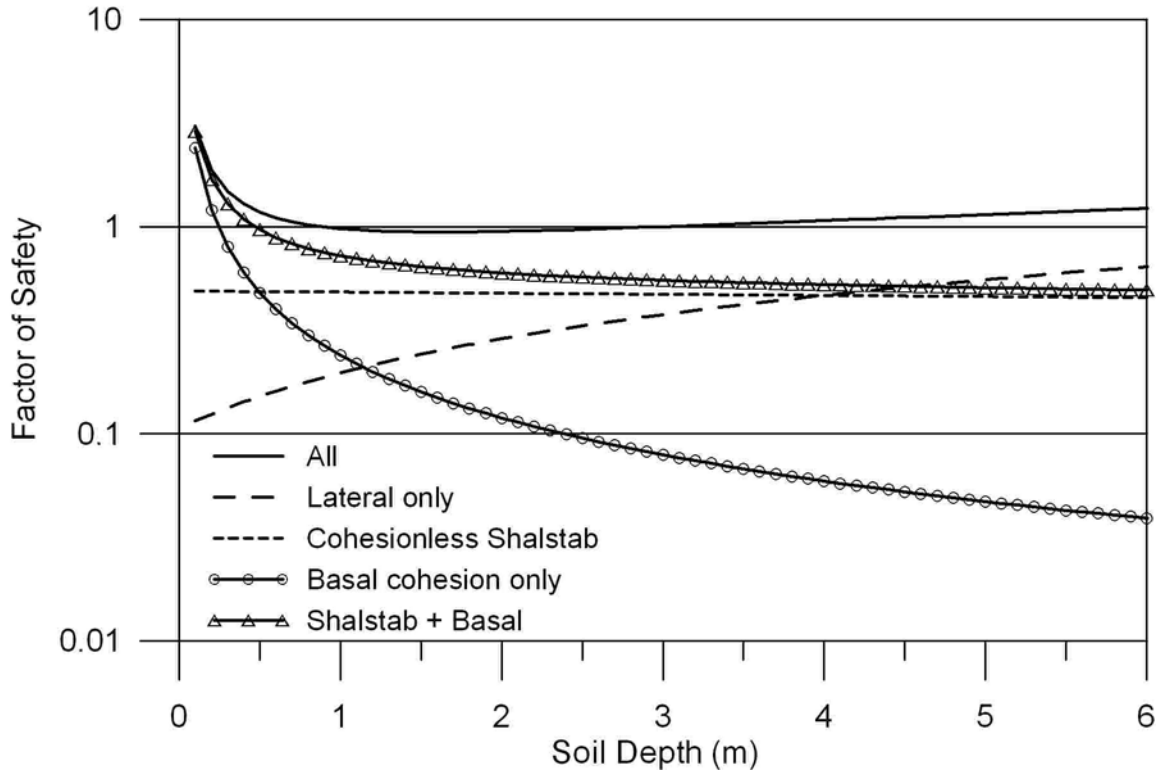


Figure 3. Contributions of basal and lateral forces to the total factor of safety. The “Shalstab only” data are from the second line in equation (1) and represent the standard infinite slope model result for cohesionless soils. The case of “Shalstab with basal cohesion” combines the first two lines in equation (1). The scenario labeled “All” includes all terms in Eq. 1. The lateral forces are the combined root cohesion and soil friction at all soil depths. The analyzed block is assumed to be 8 m wide and 16 m long, have a soil friction angle of 40° on a hillslope of 45° , and saturated conditions ($\rho_s = 1700 \text{ kg/m}^3$, $\rho_w = 1000 \text{ kg/m}^3$). Lateral root strength is 5 kPa and basal root strength is 2 kPa, but soil is otherwise cohesionless

4.2 Searching for instability

Using the soil production and transport model we can create a spatially variable field of soil depth, which, as Figs. 3 & 4 suggest, can create opportunities for slope instability to develop. For simplicity we model an inclined plane, 500 m long and 500 m wide on which we run our soil model for the equivalent of 5000 years and produce soil thicknesses that vary from 0.04 m to 1.75 m. We assume constant relative saturation, friction angle, and basal cohesion (we assume that C_b drops to zero for soils thicker than the rooting depth of 1 m) and explore two cases, one with spatially constant lateral root strength, and one with random variations in root strength.

To search for the least stable landslide mass, we developed a search algorithm that calculates the factor of safety for every possible combination of contiguous grid cells with convex boundaries (that is, the interior angles of a polygon constructed by connecting the boundary cells cannot exceed 180°). This search is computationally demanding, so we explored just a 12 by 12 cell sub-sample of the model plane of data (with 5 m grids). Even this reduction led to calculating the FS for 229,367 different configurations.

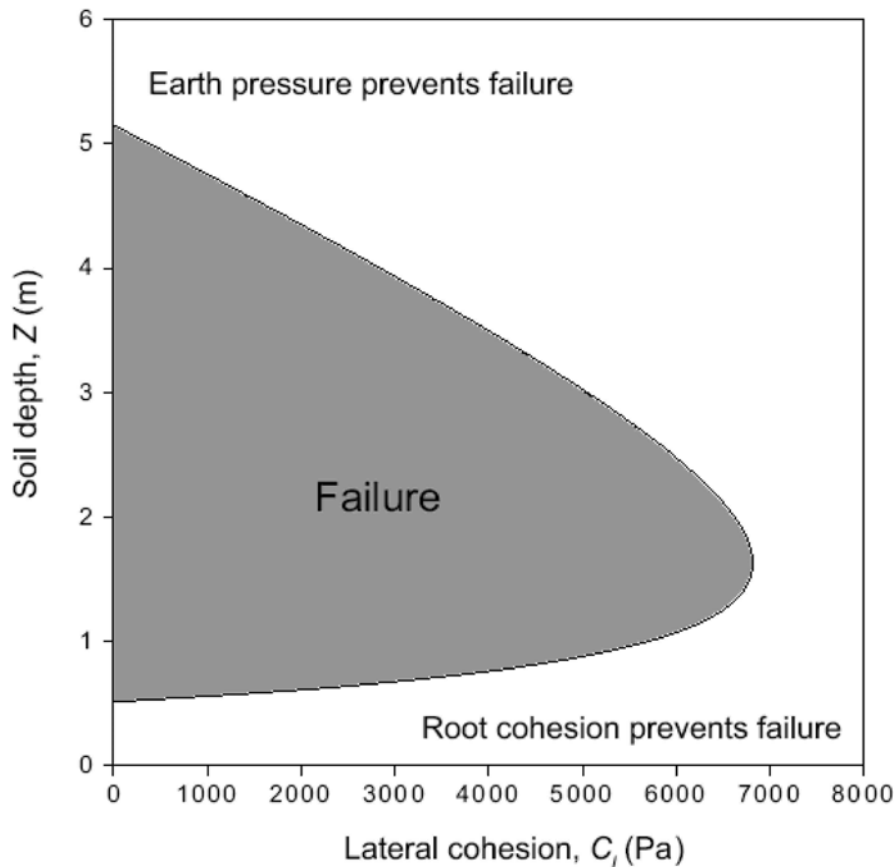


Figure 4. Stability for an 8 m wide, 16 m long soil slope element relative to soil depth and lateral root cohesion. Soil fails in conditions shown in shaded area. Basal cohesion = 2 kPa. Soil is fully saturated. Other parameters are as in Fig. 3.

Fig. 5 shows all combinations of cells that were determined to be unstable, with an emphasis on the least stable block. Lateral and basal root strength were set relatively high, such that only the largest contiguous areas of thicker soil were determined to be unstable. Next we reduced the root strength in total but introduced random patches of much higher root strength and re-ran the search. The effect was to greatly increase the number of failure blocks and the total size of failure, and to create local islands of no failure associated with the areas of high root strength.

An alternative model approach was also explored for the latter case of reduced overall root strength with patches of high strength. The search started by finding the least stable cell, removing the mass, and recalculating the stability of all cells due to the removal of that cell. The soil in the least stable cell was removed again until all unstable patches were removed. This approach, which might simulate somewhat the effects of progressive failure, resulted in a smaller number of failed cells for the chosen cell size. This result, however, does depend on cell size.

5 DISCUSSION

Lateral earth pressure increases with soil thickness, hence it is a relatively minor contributor to strength in shallow soils (where root strength predominates). Increasing soil thickness increases the lateral pressure forces such that with sufficiently thick soils, stability is generated even though root strength alone may not be sufficient to hold the soil in place. The greater the lateral root strength, however, the narrower the range of soil depth at which instability occurs. These are distinctly three-dimensional effects. These calculations suggest that when cutting or burning of the forest occurs, instability spreads to a progressively wider range of soil thickness as lateral root strength decays. This also leads to the inference that if destabilizing storms do not occur for a given vegetation cover, soils may thicken enough to cause increasing stability. This may help explain the occurrence of thick soils in buried bedrock hollows on steep hillslopes (e.g., Dietrich & Dunne 1978). The model, however, assumes that failure occurs at the soil bedrock boundary. We do observe failures above the soil bedrock boundary (e.g., Reneau & Dietrich 1987; Reneau et al. 1990). An important next step in this modeling is to allow for the failure to occur within the soil column.

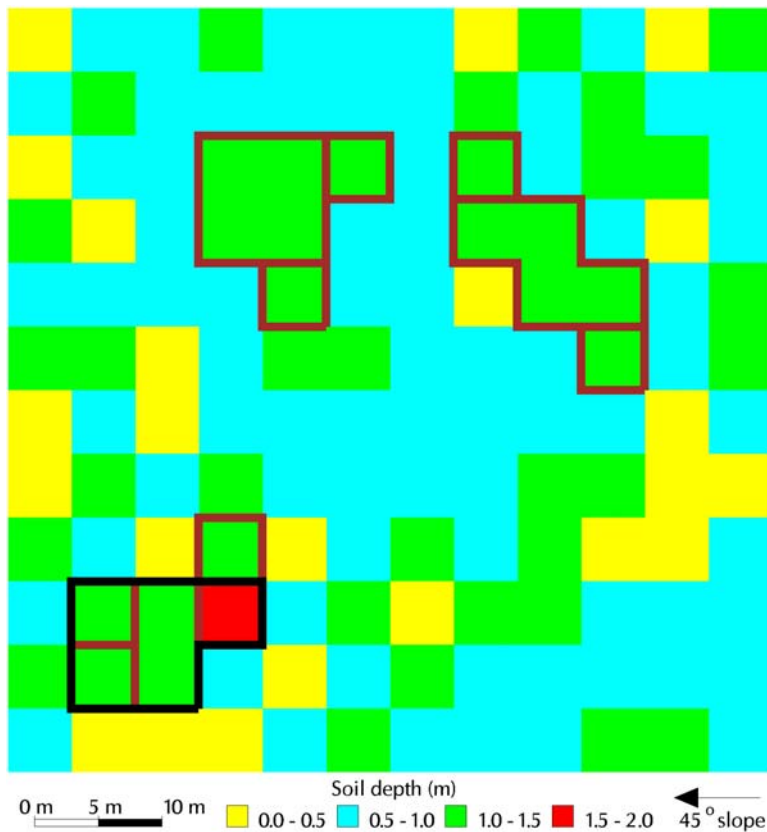


Figure 5. Pattern of soil depth, cell combinations determined to be unstable (outlined), and least stable (outlined in black) block of cells. Cell size is 5 m.

The current theory does not contradict conclusions from earlier, simpler models regarding the general controls on landslide size (e.g., Casadei & Dietrich, 2003). These models predict that the minimum possible landslide size increases with decreasing pore pressure, decreasing slope and increasing root strength. Models and high resolution remote sensing data are improving our ability to

make spatially explicit estimates of soil depth and root strength contributions (e.g., Dietrich, et al., 2001). Our soil production model emphasizes the role of biota in creating unstable material and then influencing its stability by adding root strength and varying its thickness through transport.

We generated the simplest possible hillslope geometry (inclined plane) to explore how to search for shallow landslides. Only soil depth and root strength were allowed to vary. Note, too, that our grid was parallel to the inclined plane here, something that rarely happens when applied to natural landscapes. Even with these simplifications, in order to reduce computational time, we isolated just a fraction of the hillslope for analysis. The force balance applied here can be generalized for geometries in which the grids do not follow topography (the normal case), but it may prove more productive to use cells that conform to topography, such as that developed for TOPOG (O'Loughlin 1986; Dietrich et al. 1992). Even with such a grid system, the approach of calculating all possible cell combinations and assessing their relative stability is impractical for large watersheds. This suggests that we need a more sophisticated search algorithm for detecting areas of potential instability, perhaps one that uses topographic attributes (e.g. shallow landslides don't cross divides or cross channels) to reduce the search.

6 CONCLUSIONS

Lateral earth pressure terms in a shallow slope stability model become more important with increasing soil depth, and lead to a window of potentially unstable soil thicknesses which are sufficiently great to overcome root strength and sufficiently small to not be stabilized by lateral cohesive and frictional forces. This window narrows with increasing lateral root strength. Stochastic soil production and transport may result in patches of thickened soil that can be destabilized by elevated pore pressure. Hence, it seems important to explicitly include biotic activity into models of landscape evolution involving landslides. A search algorithm in which all possible block configurations are tested for instability can be implemented on small areas, but for watershed scale applications, directed search techniques are needed to find efficiently the unstable sites.

ACKNOWLEDGMENTS

This work was supported by the USDA Forest Service, Rocky Mountain Research Station, Grant 05-JV-11221659-186 and by the STC program of the National Science Foundation via the National Center for Earth-surface Dynamics under the agreement Number EAR-0120914. Two anonymous reviews improved the manuscript.

REFERENCES

- Arellano D. & Stark, T.D. 2000. Importance of three-dimensional slope stability analysis in practice. In D.V. Griffiths, G.A. Fenton & T.R. Martin (eds.), *Slope Stability. ASCE Geotechnical Special Publication No. 101*. New York: ASCE: : 18-32.
- Benda, L.E. & Cundy, T.W. 1990. Predicting deposition of debris flows in mountain channels. *Canadian Geotechnical Journal* 27: 209-417.
- Burroughs, E.R. & Thomas, R.B. 1977. Declining root strength in Douglas-Fir after felling as a factor in slope stability. *USDA Forest Service, Intermountain Forest and Range Experiment Station, Research Paper INT-190*.
- Burroughs, E.R. 1984. Landslide hazard rating for portions of the Oregon Coast Range. In C. O'Loughlin & A.J. Pearce (eds.), *Proceedings of the Symposium on Effects of Forest Land Use on Erosion and Slope Stability. Honolulu, Hawaii, May 7-11, 1984*: 265-274.

- Casadei, M., Dietrich, W.E. & Miller, N.L. 2003. Testing a model for predicting the timing and location of shallow landslide initiation in soil mantled landscapes. *Earth Surface Processes and Landforms* 28 (9): 925-950.
- Casadei, M. & Dietrich, W.E. 2003. Controls on shallow landslide width. In D. Rickermann & C.L. Chen (eds.), *Debris-flow Hazards Mitigation: Mechanics, Prediction, and Assessment; Proceedings of the Third International DFHM Conference. Davos Switzerland, September 10-12, 2003*: 91-102.
- Chugh, A.K. 2003. On the boundary conditions in slope stability analysis. *International Journal for Numerical and Analytical Methods in Geomechanics* 27: 905-926.
- Claessens, L., Heuvelink, G.B.M., Schoorl, J.M. & Veldkamp, A. 2005. DEM resolution effects on shallow landslide hazard and soil redistribution modeling. *Earth Surface Processes and Landforms* 30: 461-477.
- Dietrich, W.E. & Dunne, T. 1978. Sediment budget for a small catchment in mountainous terrain. *Z. Geomorphologie Supplement Band* 29: 191-206.
- Dietrich, W.E., Wilson, C.J., Montgomery, D.R., McKean, J. & Bauer, R. 1992. Erosion thresholds and land surface morphology. *Geology* 20: 675-67.
- Dietrich, W.E., Reiss, R., Hsu, M. & Montgomery, D.R. 1995. A process-based model for colluvial soil depth and shallow landsliding using digital elevation data. *Hydrological Processes* 9: 383-400.
- Dietrich, W.E., Bellugi, D. & Real de Asua, R. 2001. Validation of the shallow landslide model SHALSTAB for forest management. In M.S. Wigmosta & S.J. Burges (eds.), *Land Use and Watersheds: Human influence on hydrology and geomorphology in urban and forest areas. American Geophysical Union Water Science and Application* 2: 195-227.
- Dietrich, W.E., Bellugi, D., Heimsath, A.M., Roering, J.J., Sklar, L. & Stock, J.D. 2003. Geomorphic transport laws for predicting the form and evolution of landscapes. In P. Wilcock & R. Iverson (eds.), *Prediction in Geomorphology. American Geophysical Union Monograph Series* 135: 103-132.
- Dietrich, W.E., McKean, J., Bellugi, D. & Perron, P. 2006. The prediction of landslide size using a multidimensional stability analysis. *Eos Transactions of the American Geophysical Union* 87 (52): Fall Meeting Supplement H54B-01.
- Ebel, B.A., Loague, K., Dietrich, W.E., Montgomery, D.R., Torres, R., Anderson, S.P. & Giambelluca, T.W. 2007. Near-surface hydrologic response for a steep, unchanneled catchment near Coos Bay, Oregon: 1. Sprinkling experiments. *American Journal of Science* 307: 678-708.
- Ebel, B.A., Loague, K., VanderKwaak, J.E., Dietrich, W.E., Montgomery, D.R., Torres, R. & Anderson, S.P. 2007. Near-surface hydrologic response for a steep, unchanneled catchment near Coos Bay, Oregon: 2. Physics-based simulations. *American Journal of Science* 307: 709-748.
- Fanning, R.J. & Wise, M.P. 2001. An empirical-statistical model for debris flow travel distance. *Canadian Geotechnical Journal* 38: 982-994.
- Gabet, E.J. & Dunne, T. 2002. Landslides on coastal sage-scrub and grassland hillslopes in a severe El Nino winter: The effects of vegetation conversion on sediment delivery. *Geological Society of America Bulletin* 114: 983-990.
- Gray, D.H. & Megahan, W.F. 1981. Forest vegetation removal and slope stability in the Idaho Batholith. *USDA Forest Service, Research paper* INT-271.
- Heimsath, A.M., Dietrich, W.E., Nishiizumi, K. & Finkel, R.C. 2001. Stochastic processes of soil production and transport: erosion rates, topographic variation, and cosmogenic nuclides in the Oregon Coast Range. *Earth Surface Processes and Landforms* 26: 531-552.
- Howard, A.D. 1994. A detachment-limited model of drainage basin evolution. *Water Resources Research* 30: 2261-2285.
- Hovland, H.J. 1977. Three-dimensional slope stability analysis method. *ASCE Journal of the Geotechnical Engineering Division* 103 (GT9): 971-986.
- Iverson, R.M. & Reid, M.E., 1992. Gravity-driven groundwater flow and slope failure potential: 1. Elastic effective-stress model. *Water Resources Research* 28: 925-938.
- Iverson, R.M. 2000. Landslide triggering by rain infiltration. *Water Resources Research* 36: 1897-1910.
- Montgomery, D.R. & Dietrich, W.E. 1994. A physically-based model for topographic control on shallow landsliding. *Water Resources Research* 30 (4): 1153-1171.
- Montgomery, D.R., Schmidt, K.M., Dietrich, W.E. & Greenberg H.M. 2000. Forest clearing and regional landsliding in the Pacific Northwest. *Geology* 28: 311-314.
- Okimura, T. 1994. Prediction of the shape of a shallow failure on a mountain slope: the three-dimensional multi-planar sliding surface method. *Geomorphology* 9: 223-233.

- O'Loughlin, E.M. 1986. Prediction of saturation zones in natural catchments by topographic analysis. *Water Resources Research* 22: 794-804.
- Pack, R.T., Tarboton, D.G. & Goodwin, C.N. 1998. The SINMAP approach to terrain stability mapping. In D.P. Moore & O. Hungr (eds.), *Proceedings, Eighth International Congress of the International Association for Engineering Geology and the Environment. Vancouver, Canada, September 21-25, 1998*: 1157-1165.
- Reneau, S.L. & Dietrich, W.E. 1987. Size and location of colluvial landslides in a steep forested landscape, *Proceedings of the International Symposium on Erosion and Sedimentation in the Pacific Rim. Corvallis, Oregon., August 3-7, 1987. IAHS Bulletin* 165: 39-48.
- Reneau, S.L., Dietrich, W.E., Donahue, D.J., Jull, A.J.T. & Rubin, M. 1990. Late Quaternary history of colluvial deposition and erosion in hollows, central California Coast Ranges. *Geological Society of America Bulletin* 102: 969- 982.
- Roering, J.J., Kirchner, J.W. & Dietrich, W.E. 1999. Evidence for non-linear, diffusive sediment transport on hillslopes and implications for landscape morphology. *Water Resources Research* 35: 853-870.
- Roering, J.J., Schmidt, K.M., Stock, J.D., Dietrich, W.E. & Montgomery, D.R. 2003. Shallow landsliding, root reinforcement, and the spatial distribution of trees in the Oregon Coast Range. *Canadian Geotechnical Journal* 40: 237-253.
- Rosso, R., Rulli, M.C. & Vannucchi, G. 2006. A physically based model for hydrologic control on shallow landsliding. *Water Resources Research* 42: W06410, doi: 10.1029/2005WR004369.
- Schmidt, K.M. 1999. *Root strength, colluvial soil depth, and colluvial transport on landslide-prone hillslopes*. Ph.D thesis. Seattle: University of Washington.
- Schmidt, K.M., Roering, J.J., Stock, J.D., Dietrich, W.E., Montgomery, D.R. & Schaub, T. 2001. Root cohesion variability and shallow landslide susceptibility in the Oregon Coast Range. *Canadian Geotechnical Journal* 38 (1): 995-1024.
- Schulz, W.H. 2006. Landslide susceptibility revealed by LIDAR imagery and historical records, Seattle, Washington. *Engineering Geology* 89: 67-87.
- Soeters, R. & van Westen, C.J. 1996. Slope instability recognition, analysis, and zonation. In A.K. Turner & R.L. Schuster (eds.), *Landslides: Investigation and Mitigation; U.S. National Research Council, Transportation Research Board, Special Report 247*. Washington D.C.: National Academy Press: 129-177.
- Tarolli, P. & Tarboton, D.G. 2006. A new method for determination of most likely landslide initiation points and the evaluation of digital terrain model scale in terrain stability mapping. *Hydrology and Earth System Science* 10: 663-377.
- Tucker, G.E. & Bras, R.L. 1998. Hillslope processes, drainage density, and landscape morphology. *Water Resources Research* 34: 2751-2764.
- Wu, W. & Sidle, R.C. 1995. A distributed slope stability model for steep forested basins. *Water Resources Research* 31: 2097-2110.
- Xie, M., Esaki, T. & Zhou, G. 2004. GIS-based probabilistic mapping of landslide hazard using a three dimensional deterministic model. *Natural Hazards* 33: 265-282.
- Xie, M., Esaki, T. & Cai, M. 2006. GIS-based implementation of three-dimensional limit equilibrium approach of slope stability. *Journal of Geotechnical and GeoEnvironmental Engineering* 132: 656-660.
- Ziemer, R.R. 1981. Roots and the stability of forested slopes. In T.R.H. Davies & A.J. Pearce (eds.), *Erosion and Sediment Transport in Pacific Rim Steeplands. International Association of Hydrological Sciences* 132: 343-361.